Design of electron band-pass filters for semiconductor superlattices.

G. V. Morozov and D. W. L. Sprung
Department of Physics and Astronomy, McMaster University
Hamilton, Ontario L8S 4M1 Canada

J. Martorell
Departament d'Estructura i Constituents de la Materia, Facultat Física, University of Barcelona
Barcelona 08028, Spain

(August 19, 2002)

We design an N-cell anti-reflection coating for electron transport through an arbitrary periodic semiconductor heterostructure. Stability conditions are derived which allow one to make an N'th order zero of the reflection amplitude at the design energy. Examples are given for up to $N = 4$ cells, showing that 95 % average transmissivity can be obtained. **Version of 2002/08/19.**

I. INTRODUCTION

Recently [1] we considered the design of an efficient energy band-pass filter for electrons in a semiconductor superlattice, inspired by the recent work of Pacher et al. [2]. We derived analytical expressions for the parameters of the additional potentials (antireflection coating or ARC) that can be added at both ends of an arbitrary periodic structure in order to achieve optimal transmission through the allowed band, treating the ARC as a single entity. In the present paper we extend our analysis by taking the ARC to consist of any number N of additional cells. This allows for significant improvement in the device properties. As before, the aim is to develop a general analytical method for the construction of an ARC which optimizes transmission through the allowed band. More generally, the aim is to understand the factors which facilitate the transport of electrons through layered devices, of which quantum cascade lasers are an important example.

Two important aspects of our method are these: First, we use a general parameterization of the transfer matrix for symmetric potentials (which was invented by Kard [3] for square potentials only). This separates the problem into two parts, one being to find the optimal values of the transfer matrix parameters, and the other, to find the precise form of a cell potential that reproduces these required values. Second, as in our previous article [1], we concentrate on the envelope of minima of the transmission resonances, avoiding the complications associated with the rapidly oscillating transmission amplitude within an allowed band.

In section II we extend the results of reference [1], to the present case. In section III we outline the general method for obtaining an optimal N-cell ARC, which is developed for the specific cases of two to four cells in section IV. Numerical examples given in the remaining section show that our method produces better performance than the fifteen cell gaussian recipe of Gomez et al. [4], with half the number of cells. Our examples show that transmissivity across the allowed band can reach 95%.

II. THEORY AND METHOD

In the single-band envelope function approximation, the electron wavefunction satisfies the Schrödinger equation including a position-dependent effective mass. We consider an *arbitrarily shaped* real symmetric potential $v(x)$ which consists of three parts. The core or central part is a periodic repetition (denoted $v_{c^K}(x)$) of $v_c(x)$ repeated K times, on the interval $0 < x < Kd$. We denote the additional potentials on each side of the periodic structure as $v_i(x)$ and $v_f(x)$ respectively. To ensure reflection symmetry of the augmented potential, $v_f(x)$ must be the mirror image of the potential $v_i(x)$, while $v_c(x)$ must be reflection symmetric itself. A schematic drawing of such a structure is shown in Fig. 1. The corresponding transfer matrices are denoted C for $v_c(x)$, C^K for $v_{c^K}(x)$, and A, A^π for the potentials $v_i(x)$, $v_f(x)$ respectively. The transfer matrix M for the total structure is

$$M = A\, C^K\, A^\pi\,. \tag{1}$$

The matrix A for any real potential can be written in terms of its reflection and transmission amplitudes r_a and t_a as [5]

$$A = \begin{pmatrix} a_{11} & a_{12} \\ a_{21} & a_{22} \end{pmatrix} = \begin{pmatrix} 1/t_a & r_a^*/t_a^* \\ r_a/t_a & 1/t_a^* \end{pmatrix}\,. \tag{2}$$

The matrix C is expressed similarly with replacement of $a \to c$ throughout. For the mirror matrix $A^\pi = (A^{-1})^*$ we have

$$A^\pi = \begin{pmatrix} a_{11} & -a_{21} \\ -a_{12} & a_{22} \end{pmatrix} = \begin{pmatrix} 1/t_a & -r_a/t_a \\ -r_a^*/t_a^* & 1/t_a^* \end{pmatrix}\,. \tag{3}$$

If in addition the potential takes a constant value outside the region where the foregoing potentials are defined, then conservation of flux implies that both $\det C = 1$ and $\det A = 1$.

The transfer matrix depends on two complex amplitudes, but the condition on $\det C$ leaves just three real

parameters in general. As our unit cell $v_c(x)$ is reflection symmetric, the elements c_{21} and c_{12} are purely imaginary, which makes $c_{12} = -c_{21}$, leaving just two independent real parameters at a given energy. We take one to be the Bloch phase associated with the infinitely periodic potential whose unit cell is $v_c(x)$: $\cos\phi_c = (c_{11}+c_{22})/2 = \Re(1/t_c)$. It is then easily seen that in an allowed band we can write [3]

$$C = \begin{pmatrix} \cos\phi_c - i\cosh\mu_c \sin\phi_c & i\sinh\mu_c\sin\phi_c \\ -i\sinh\mu_c\sin\phi_c & \cos\phi_c + i\cosh\mu_c\sin\phi_c \end{pmatrix} \tag{4}$$

The parameters $\phi_c(E)$ and $\mu_c(E)$ depend on the electron energy and on the properties of the potential $v_c(x)$. In allowed bands ($-1 < \cos\phi_c < 1$) both parameters are real. We can call μ_c an impedance parameter, because in the case of a flat potential, $\mu_c = \log Z$, where Z is the inverse velocity in that potential [6]. Numerical examples in section 4 show that μ_c is approximately constant while $\cos\phi_c$ depends almost linearly on energy across much of each allowed band,

Transmission through the total system including the ARC and K central cells can be expressed in terms of the off-diagonal element M_{21} of the total transfer matrix M as

$$|T_K|^2 = \frac{1}{1+|M_{21}|^2}\,. \tag{5}$$

After some algebra we express the element $|M_{21}|^2$ in the form

$$|M_{21}|^2 = \left|\alpha^2 - 2\alpha\beta\cos\phi_c + \beta^2\right| \left|\frac{\sin(K\phi_c+\delta)}{\sin\phi_c}\right|^2\,, \tag{6}$$

where the complex parameters α, β, and δ are combinations of elements of the matrices C and A:

$$\begin{aligned} \alpha &= a_{21}a_{11}c_{11} - a_{12}a_{22}c_{22} + (a_{11}a_{22}+a_{21}a_{12})c_{21}\,, \\ \beta &= a_{21}a_{11} - a_{12}a_{22}\,, \quad \tan\delta = \frac{\beta\sin\phi_c}{\alpha - \beta\cos\phi_c}\,. \end{aligned} \tag{7}$$

(If the mirror potential $v_f(x)$ is simply identical to $v_i(x)$, as in Ref. [1], there is an additional simplification $a_{12} = -a_{21}$.) Eqs. (6) and (7) are valid for any potential, but in our case of overall reflection symmetry, the parameters α and β become pure imaginary, and δ real. This allows us to obtain the envelope of transmission minima in allowed bands, which is a curve independent of K, by setting the factor $\sin^2(K\phi+\delta) \to 1$ in eq. (6).

$$|T|^2_{min} = \frac{1}{1+\left|\alpha^2 - 2\alpha\beta\cos\phi_c + \beta^2\right| / \sin^2\phi_c}\,. \tag{8}$$

Finally, we define the average transmissivity τ for electrons passing within the allowed band as

$$\tau = \frac{1}{(E_h - E_l)}\int_{E_l}^{E_h} |T_K|^2 dE\,. \tag{9}$$

where E_l, E_h are the lower and upper band edges. The ideal filter would have transmissivity $\tau = 1$ in the allowed band, and $|T_K|^2 = 0$ in forbidden bands. The second requirement is well satisfied when the number of periods K is large; in [1] we showed that $K = 5$ is already sufficient.

III. GENERAL REQUIREMENTS FOR ANTIREFLECTION COATINGS

Here we study conditions on the additional potentials $v_i(x)$ and $v_f(x)$ which will provide the highest possible transmissivity through the allowed band. By making the envelope of minima eq. (8) reach perfect transmission somewhere near the center of the allowed band, we already obtain a reasonable transmission profile, since the first derivative of $|T^2|_{min}$ is also zero at this point. This ensures that deviations of $|T_K|^2$ from unity are small except close to the zone boundaries, where transmission necessarily tends to zero. The specific design energy E_b where we will force perfect transmission is the Bragg energy of the cell $v_c(x)$ where $\cos\phi_c(E_b) = 0$, i.e. $\phi_c(E_b) = \pi/2$. Other choices are possible, and sometimes preferable, for example the exact mid-point of the band, i.e. $E_m = (E_l + E_h)/2$, as in Ref. [1].

To make the envelope touch unity at energy E_b, it is necessary and sufficient that both $\beta = 0$ and $\alpha = 0$ at this point. As a result, the elements of the transfer matrix A for the ARC coating $v_i(x)$ must satisfy two conditions:

$$\begin{aligned} &a_{21}(E_b)a_{11}(E_b) - a_{12}(E_b)a_{22}(E_b) = 0 \\ &\frac{a_{22}(E_b)}{a_{21}(E_b)} + \frac{a_{12}(E_b)}{a_{11}(E_b)} + 2\coth\mu_c(E_b) = 0\,. \end{aligned} \tag{10}$$

Now we turn to the detailed internal structure of the ARC layer $v_i(x)$. For application to semiconductor heterostructures, we can consider the device to consist of a finite number of homogeneous layers. These can be grouped into a (generally smaller) number N of reflection symmetric cells. We denote the potential in the p'th cell by $a_p(x)$ and the corresponding transfer matrix by A_p. The matrix A becomes a product

$$A = \prod_{p=N}^{1} A_p\,, \quad \text{where } A_p = \begin{pmatrix} \cos\phi_p - i\cosh\mu_p\sin\phi_p & i\sinh\mu_p\sin\phi_p \\ -i\sinh\mu_p\sin\phi_p & \cos\phi_p + i\cosh\mu_p\sin\phi_p \end{pmatrix} \tag{11}$$

One way (see the Appendix) to satisfy the first equation in (10) is to take all $\cos\phi_p(E_b) = 0$, i.e.

$$\phi_p(E_b) = \pi/2\,, \quad p = 1, 2 \ldots N\,. \tag{12}$$

Such an ARC is called a quarter-wavelength coating and the energy E_b (design energy for the ARC) becomes a common Bragg point for the ARC cells. Eq. 11 then reduces to

$$A(E_b) = \prod_{p=N}^{1} \begin{pmatrix} -i\cosh\mu_p & i\sinh\mu_p \\ -i\sinh\mu_p & i\cosh\mu_p \end{pmatrix}, \qquad (13)$$

where all μ_p are taken at the energy E_b. This can be evaluated as

$$A(E_b) = \begin{pmatrix} (-i)^N\cosh\mu_a & i^N\sinh\mu_a \\ (-i)^N\sinh\mu_a & i^N\cosh\mu_a) \end{pmatrix}, \quad \text{where}$$
$$\mu_a = \sum_{p=1}^{N}(-1)^{N-p}\mu_p \qquad (14)$$

is the impedance parameter μ_a for the complete ARC coating $v_i(x)$ at energy E_b. The second equation in (10) then leads to the requirement

$$\mu_a = (-)^{N-1}\mu_c/2\,. \qquad (15)$$

According to eqs. (12) and (15), if the ARC coating $v_i(x)$ consists of a single cell $a_1(x)$, its parameters are

$$\phi_1(E_b) = \pi/2\,, \quad \mu_1 = \mu_c/2. \qquad (16)$$

This is the result of [1]. (For $N = 1$, taking the ARC to be a Bragg reflector is not a choice, but necessary, as shown in [1].)

For $N > 1$ cells, eqs. (12) and (15) do not define a unique solution, and we use this freedom to impose additional conditions on μ_p, to maintain the highest possible transmission at nearby energies, i.e. to make the envelope of minima as flat as possible around the design energy E_b. In order to achieve this, we should keep the conditions (10) approximately valid at selected energies E_j close to E_b, for which we can write $\phi_p(E_j) = \pi/2 - \epsilon_p$, where all $\epsilon_p(E_j)$ are small. In addition we will assume that $\mu_p(E_j) = \mu_p(E_b)$, as $\mu_p(E)$ changes very slowly with energy in the middle of an allowed band. With these approximations, eq. (11) becomes

$$A(E_j) = \prod_{p=N}^{1} A_p(E_j)\,, \quad \text{with}$$
$$A_p(E_j) = \sin\epsilon_p\, I + \cos\epsilon_p\, A_p(E_b), \qquad (17)$$

where I is the unit matrix, and ϵ_p is evaluated at E_j in what follows. The result of expanding the elements of $A(E_j)$ in powers of the small parameters ϵ_p, is written as

$$i^N\, a_{11}(E_j) = \cosh\mu_a + \sum_{k=1}^{N-1} i^k\, x_k\ ,$$
$$i^N\, a_{21}(E_j) = \sinh\mu_a + \sum_{k=1}^{N-1} i^k\, y_k\ , \qquad (18)$$

where we denote the sum of all terms of k-th order by x_k for the element $a_{11}(E_j)$ and by y_k for the element $a_{21}(E_j)$. Applying the conditions (10) at the point E_j, leads to $(N-1)$ additional equations of the form

$$y_k\cosh\mu_a - (-1)^k\, x_k\, \sinh\mu_a = 0\,, \qquad (19)$$

with $k = 1 \ldots (N-1)$. For the N-cell ARC we have $2N$ independent parameters $\phi_N \ldots \phi_1$, $\mu_N \ldots \mu_1$, and $2N$ equations, of which $N+1$ are assigned to make the envelope of minima reach perfect transmission at the design energy (eqs. (12) and (15)). The remaining $(N-1)$ (eq. 19) we call stability conditions because we use them to make the envelope of transmission minima as flat as possible around the design energy. In the next section we develop this method for some specific cases.

IV. DOUBLE , TRIPLE, AND QUADRUPLE CELL ANTIREFLECTION COATINGS

A. Double cell ARC

Suppose the potential $v_i(x)$ consists of two symmetrical cells $a_2(x)$ and $a_1(x)$ with their corresponding transfer matrices A_2 and A_1. In this case we have two parameters μ_2 and μ_1 to optimize transmission through the allowed band, in accordance with eqs. (12) and (15)

$$\pi/2 = \phi_2(E_b) = \phi_1(E_b)\,,$$
$$\mu_c/2 = \mu_1 - \mu_2\,. \qquad (20)$$

Using expressions (17) and (18) with $N = 2$, we obtain

$$x_1 = \epsilon_1\cosh\mu_2 + \epsilon_2\cosh\mu_1\,,$$
$$y_1 = \epsilon_1\sinh\mu_2 + \epsilon_2\sinh\mu_1\,. \qquad (21)$$

The resulting stability condition for this case eq. (19) takes the form

$$\epsilon_1\sinh(2\mu_2 - \mu_1) + \epsilon_2\sinh\mu_2 = 0\,. \qquad (22)$$

We should emphasize that the shape of the cell potentials $a_p(x)$ can be very complicated, but so long as its parameters ϕ_p and μ_p take the required values, one will have the desired performance. It is a separate matter, (see section IV), to choose the actual cell potential shape. In the case of optical or microwave filters, usually one treats each layer as a cell. Then it is possible to arrange that $\phi_1 = \phi_2$ (more generally, all ϕ_k are equal) at all wavelengths (energies) for normal incidence. This is called making the layers of equal optical depth. Then, all the ϵ_k are equal. In that circumstance, eq. 22 leads to the solution $\mu_1 = 3\mu_2$, which is the well-known Butterworth or maximally flat filter design. In contrast, for electrons in semiconductors, one cannot assume that the ϵ_k are equal, and the solution can be quite different. This is the principal difference between filters for electrons, and the classic designs, and it has not been considered in previous work, such as [6], which assumed the classic filters to be valid.

B. Three cell ARC

In this case we have three Bragg cells and require

$$\mu_c/2 = \mu_1 - \mu_2 + \mu_3. \tag{23}$$

The expansion terms in (18) take the form

$$\begin{aligned}
x_1 &= \epsilon_1 \cosh(\mu_3 - \mu_2) + \epsilon_2 \cosh(\mu_3 - \mu_1) + \epsilon_3 \cosh(\mu_2 - \mu_1)\,, \\
y_1 &= \epsilon_1 \sinh(\mu_3 - \mu_2) + \epsilon_2 \sinh(\mu_3 - \mu_1) + \epsilon_3 \sinh(\mu_2 - \mu_1)\,, \\
x_2 &= \epsilon_1\epsilon_2 \cosh\mu_3 + \epsilon_1\epsilon_3 \cosh\mu_2 + \epsilon_2\epsilon_3 \cosh\mu_1 \\
&\quad + \frac{\epsilon_1^2 + \epsilon_2^2 + \epsilon_3^2}{2} \cosh(\mu_1 - \mu_2 + \mu_3)\,, \\
y_2 &= \epsilon_1\epsilon_2 \sinh\mu_3 + \epsilon_1\epsilon_3 \sinh\mu_2 + \epsilon_2\epsilon_3 \sinh\mu_1 \\
&\quad + \frac{\epsilon_1^2 + \epsilon_2^2 + \epsilon_3^2}{2} \sinh(\mu_1 - \mu_2 + \mu_3)
\end{aligned} \tag{24}$$

and the two stability conditions from (19) ($N = 3$) are

$$\begin{aligned}
0 &= \epsilon_1 \sinh(\mu_1 - 2\mu_2 + 2\mu_3) + \epsilon_2 \sinh(2\mu_3 - \mu_2) + \epsilon_3 \sinh\mu_3\,, \\
0 &= \epsilon_1\epsilon_2 \sinh(\mu_1 - \mu_2) + \epsilon_2\epsilon_3 \sinh(\mu_3 - \mu_2) + \epsilon_1\epsilon_3 \sinh(\mu_1 - 2\mu_2 + \mu_3)\,.
\end{aligned} \tag{25}$$

Under these stability conditions contributions to the reflection which are linear or quadratic in ϵ_p will vanish at nearby energies E_j.

C. Four cell ARC

Finally, we consider the case when the potential $v_i(x)$ consists of four symmetrical cells $a_4(x)$, $a_3(x)$, $a_2(x)$, and $a_1(x)$. According to (12) and (15), the eight basic parameters at hand are related by

$$\begin{aligned}
\pi/2 &= \phi_4(E_b) = \phi_3(E_b) = \phi_2(E_b) = \phi_1(E_b)\,, \\
\mu_c/2 &= \mu_1 - \mu_2 + \mu_3 - \mu_4.
\end{aligned} \tag{26}$$

The expansion terms in (18) take the form

$$\begin{aligned}
y_1 &= \epsilon_1 \sinh(\mu_4 - \mu_3 + \mu_2) + \epsilon_2 \sinh(\mu_4 - \mu_3 + \mu_1) \\
&\quad + \epsilon_3 \sinh(\mu_4 - \mu_2 + \mu_1) + \epsilon_4 \sinh(\mu_3 - \mu_2 + \mu_1)\,, \\
y_2 &= \epsilon_1\epsilon_2 \sinh(\mu_4 - \mu_3) + \epsilon_1\epsilon_3 \sinh(\mu_4 - \mu_2) + \epsilon_1\epsilon_4 \sinh(\mu_3 - \mu_2) \\
&\quad + \epsilon_2\epsilon_3 \sinh(\mu_4 - \mu_1) + \epsilon_2\epsilon_4 \sinh(\mu_3 - \mu_1) + \epsilon_3\epsilon_4 \sinh(\mu_2 - \mu_1) \\
&\quad + \frac{\epsilon_1^2 + \epsilon_2^2 + \epsilon_3^2 + \epsilon_4^2}{2} \sinh(\mu_4 - \mu_3 + \mu_2 - \mu_1)\,, \\
y_3 &= \epsilon_1\epsilon_2\epsilon_3 \sinh\mu_4 + \epsilon_1\epsilon_2\epsilon_4 \sinh\mu_3 + \epsilon_1\epsilon_3\epsilon_4 \sinh\mu_2 + \epsilon_2\epsilon_3\epsilon_4 \sinh\mu_1 \\
&\quad + \epsilon_1 \left(\frac{\epsilon_2^2 + \epsilon_3^2 + \epsilon_4^2}{2}\right) \sinh(\mu_4 - \mu_3 + \mu_2) + \epsilon_2 \left(\frac{\epsilon_1^2 + \epsilon_3^2 + \epsilon_4^2}{2}\right) \sinh(\mu_4 - \mu_3 + \mu_1) \\
&\quad + \epsilon_3 \left(\frac{\epsilon_1^2 + \epsilon_2^2 + \epsilon_4^2}{2}\right) \sinh(\mu_4 - \mu_2 + \mu_1) + \epsilon_4 \left(\frac{\epsilon_1^2 + \epsilon_2^2 + \epsilon_3^2}{2}\right) \sinh(\mu_3 - \mu_2 + \mu_1) \\
&\quad + \frac{\epsilon_1^3}{6} \sinh(\mu_4 - \mu_3 + \mu_2) + \frac{\epsilon_2^3}{6} \sinh(\mu_4 - \mu_3 + \mu_1) \\
&\quad + \frac{\epsilon_3^3}{6} \sinh(\mu_4 - \mu_2 + \mu_1) + \frac{\epsilon_4^3}{6} \sinh(\mu_3 - \mu_2 + \mu_1)\,.
\end{aligned} \tag{27}$$

The parameters x_1, x_2, and x_3 are expressed similarly with replacement of $\sinh \to \cosh$ throughout.

The three stability conditions (19) ($N = 4$) take the form

$$
\begin{aligned}
0 &= \epsilon_1 \sinh(2\mu_4 - 2\mu_3 + 2\mu_2 - \mu_1) + \epsilon_2 \sinh(2\mu_4 - 2\mu_3 + \mu_2) \\
&\quad + \epsilon_3 \sinh(2\mu_4 - \mu_3) + \epsilon_4 \sinh \mu_4 \,, \\
0 &= \epsilon_1\epsilon_2 \sinh(\mu_1 - \mu_2) + \epsilon_1\epsilon_3 \sinh(\mu_1 - 2\mu_2 + \mu_3) + \epsilon_1\epsilon_4 \sinh(\mu_1 - 2\mu_2 + 2\mu_3 - \mu_4) \\
&\quad + \epsilon_2\epsilon_3 \sinh(\mu_3 - \mu_2) + \epsilon_2\epsilon_4 \sinh(-\mu_2 + 2\mu_3 - \mu_4) + \epsilon_3\epsilon_4 \sinh(\mu_3 - \mu_4) \,, \\
0 &= \epsilon_1\epsilon_2\epsilon_3 \sinh(2\mu_4 - \mu_3 + \mu_2 - \mu_1) + \epsilon_1\epsilon_2\epsilon_4 \sinh(\mu_4 + \mu_2 - \mu_1) \\
&\quad + \epsilon_1\epsilon_3\epsilon_4 \sinh(\mu_4 - \mu_3 + 2\mu_2 - \mu_1) + \epsilon_2\epsilon_3\epsilon_4 \sinh(\mu_4 - \mu_3 + \mu_2) \\
&\quad + \epsilon_1 \left(\frac{\epsilon_2^2 + \epsilon_3^2 + \epsilon_4^2}{2} \right) \sinh(2\mu_4 - 2\mu_3 + 2\mu_2 - \mu_1) + \epsilon_2 \left(\frac{\epsilon_1^2 + \epsilon_3^2 + \epsilon_4^2}{2} \right) \sinh(2\mu_4 - 2\mu_3 + \mu_2) \\
&\quad + \epsilon_3 \left(\frac{\epsilon_1^2 + \epsilon_2^2 + \epsilon_4^2}{2} \right) \sinh(2\mu_4 - \mu_3) + \epsilon_4 \left(\frac{\epsilon_1^2 + \epsilon_2^2 + \epsilon_3^2}{2} \right) \sinh \mu_4 \\
&\quad + \frac{\epsilon_1^3}{6} \sinh(2\mu_4 - 2\mu_3 + 2\mu_2 - \mu_1) + \frac{\epsilon_2^3}{6} \sinh(2\mu_4 - 2\mu_3 + \mu_2) \\
&\quad + \frac{\epsilon_3^3}{6} \sinh(2\mu_4 - \mu_3) + \frac{\epsilon_4^3}{6} \sinh \mu_4 \,.
\end{aligned}
\tag{28}
$$

Under these stability conditions linear, quadratic and cubic terms in the reflection amplitude will vanish at nearby energies E_j.

The last piece of information we require, to solve the above systems of equations, is the relative values of the set of ϵ_p for $p \in 1...N$. Because the stability conditions are homogeneous, it is only the ratios of the ϵ_p that matter. For electrons in semiconductors the curves for the $\cos\phi_p$ are almost linear near the Bragg point E_b; see Fig. 2. This allows us to approximate

$$
\cos\phi_p(E_j) \simeq \cos\phi_p(E_b) + (\cos(\phi_p(E))'_{E=E_b}(E_j - E_b). \tag{29}
$$

As $\phi_p(E_j) = \phi_p(E_b) - \epsilon_p$, where all ϵ_p are small, eq. (29) takes the form

$$
\epsilon_p \simeq (\cos(\phi_p(E))'_{E=E_b}(E_b - E_j). \tag{30}
$$

Therefore, the ratios of the ϵ_p are approximately equal to the ratios of the slopes of the $\cos\phi_p$ curves at the Bragg point E_b. These in turn depend on the properties of the chosen ARC cells. Fig. 2 shows that this approximation works well over most of the allowed band of the central periodic structure $v_{cK}(x)$. The example shown is for a three-cell filter, and the slopes are in ratio 0.38 : 0.67 : 0.93 : 1.0, the last figure being the central cells.

As a very rough working rule, we find that the ratio of slopes at the Bragg point is approximately the ratio of the barrier strengths, *i.e.* to $S_p = \sqrt{V_p}\, b_p$ in case of a square barrier cell. Note that according to the above argument, the stability conditions apply not at some specific energy E_j, but over a range of energies where the $\cos\phi_p$ curves maintain constant ratios. Fig. 2 shows that this is a large part of the allowed band.

V. NUMERICAL EXAMPLES

We first consider an energy band pass filter consisting of a row of delta-functions of strength V_0 and spacing d as the periodic medium. This is relevant to devices such as that of Gomez et al. [4], where the barriers are strong but thin. The transfer matrix C can be written in the form [5]

$$
C = \begin{pmatrix} (1 + i\Omega_c/k)\, e^{-ikd} & i\Omega_c/k \\ -i\Omega_c/k & (1 - i\Omega_c/k)\, e^{ikd} \end{pmatrix} \,, \tag{31}
$$

where $k^2 = 2m^*E/\hbar^2$, $\Omega_c = m^*V_0/\hbar^2$, and m^* is the effective mass of an electron. Then the Bloch phase ϕ_c and the parameter μ_c are given by (see eq. (4)),

$$
\begin{aligned}
\cos\phi_c &= \cos kd + \frac{\Omega_c}{k} \sin kd \,, \\
\tanh\mu_c &= \frac{\Omega_c}{k \sin kd - \Omega_c \cos kd} \,.
\end{aligned}
\tag{32}
$$

The parameters Ω_c and d are determined by the desired band edges: $\cos\phi_c(k_l) = 1$, and $\cos\phi_c(k_h) = -1$. These lead to

$$
d = \pi/k_h \,, \quad \Omega_c = k_l \tan(k_l d/2) \,. \tag{33}
$$

We construct the antireflection coating from delta-potential cells as well. Such a cell is described by just two parameters, so ϕ_p and μ_p for the cell fix its parameters uniquely.

If there is only one cell in the coating ($N = 1$), eq. (16) easily determines parameters μ_1 and $\phi_1(E_b)$ of this cell. Then, we can find the cell width d_1 and the strength Ω_1, using the expressions (32) at the point $E = E_b$, in which one should replace Ω_c by Ω_1, d by d_1, ϕ_c by ϕ_1, and μ_c by μ_1. If there are two, three, or four cells in the ARC coating, in order to find the best solution, we should impose the stability conditions (22), (25), or (28), taking into account (30).

As a specific example, we place the first allowed band at 122 meV $< E <$ 172 meV. The resulting parameters are $\Omega_c = 1.88$ nm^{-1} and $d = 5.55$ nm; the strength $V_0 = \hbar^2\Omega_c/m^*$ is 590 meV nm for constant $m^* = 0.071 m_e$.

Our solutions for different numbers of ARC cells in the coating are shown in Table I, while the corresponding transmission curves are shown in Fig. 3. In each example, the ARC produces a significant improvement compared to the initial periodic structure. The average transmissivities are $\tau = 0.21$ for the initial superlattice, $\tau = 0.80$ with a single-cell ARC; $\tau = 0.91$ for the double cell coating, $\tau = 0.95$ for the triple cell coating, and $\tau = 0.96$ for the quadruple. Note that the envelope of minima of the augmented lattice gets rapidly wider as N increases; this is what pushes up the $|T_K|^2$ curve towards unity. If the number of central cells K were increased, the transmission curve would show additional oscillations above the *same* envelope of minima.

As a second example of our theory, we consider a bandpass filter based on a square barrier superlattice. Gomez et al. [4] proposed a 15 cell filter based on a gaussian distribution of barrier heights. This is illustrated in the top row of Fig. 4. Such a model had been studied earlier by Tung and Lee [7,8], who argued that a smoothly rising profile should reduce reflection. One could question how this applies to a sequence of square barriers of height $V_b > E > V_w$. Subsequently, Yang and Li [9] carried out similar calculations, choosing a variety of different distributions. In neither case was a sound theory advanced to explain why such an array should have favourable transmission properties. We will limit our discussion and comparisons to the Gomez example.

In the notation of Fig. 1, the barriers are of height V, width b, and separated by w. To make symmetric cells, we include a half-well on each side of each barrier. The transfer matrix C has elements [2]

$$\begin{aligned} c_{11} &= (\cos\beta b - iZ^{(+)}\sin\beta b)e^{-ikw} = c_{22}^* \\ c_{21} &= -iZ^{(-)}\sin\beta b \ = c_{12}^* \end{aligned} \tag{34}$$

where $Z^{(\pm)} = (k^2 \pm \beta^2)/(2k\beta)$, and $k^2 = 2m^*E/\hbar^2$, $\beta^2 = 2m^*(E-V)/\hbar^2$. The dispersion equation for the Bloch phase ϕ_c and the parameter μ_c are given by

$$\begin{aligned} \cos\phi_c &= \cos\beta b \ \cos kw \ - Z^{(+)}\sin\beta b \ \sin kw \ , \\ \tanh\mu_c &= \frac{Z^{(-)}\sin\beta b}{\cos\beta b \ \sin kw \ + Z^{(+)}\sin\beta b \ \cos kw} \, . \end{aligned} \tag{35}$$

In the gaussian array of ref. [4], the core potential $v_{c^K}(x)$ is a single square barrier cell, $K = 1$, of height $V = 350$ meV, corresponding to an $Al_{0.45}Ga_{0.55}As/GaAs$ superlattice. They took the effective mass to be 0.067 in both well and barrier, neglecting material and energy dependence. We will adopt their parameters to facilitate comparison. To construct our filter we use a periodic structure with $K = 3$ such central cells. Using the first of the eqs. (35) we obtain the first allowed band from 47.7 meV $< E <$ 98.5 meV. At the Bragg point $E_b = 66.8$ meV the second of the eqs. (35) determines $\mu_c = 1.26$.

To construct the ARC we also use square barrier cells. To provide the required values of $\cos\phi_p$ and μ_p for each cell, we have three parameters V_p (the barrier height), b_p (the barrier width), and w_p (the well width) at hand. One possible set of resulting parameters is shown in Table II and the corresponding transmission curves in Fig. 5. We show results for (a) $N = 1$ and (b) $N = 4$ cells, and it is seen that they are similar to the earlier example. The average transmissivities are $\tau = 0.41$ for the initial superlattice, $\tau = 0.81$ with a single cell coating, $\tau = 0.90$ with a double cell coating, $\tau = 0.93$ with a triple cell coating, and $\tau = 0.95$ with a quadruple cell coating. In general, the results parallel those of the delta model. The transmission through the first allowed band of the augmented system is much higher than for the periodic structure alone. The envelope of minima for the augmented system is also shown; if more than $K = 3$ central cells were included, the transmission curve would oscillate above that line.

The gaussian filter of ref. [4] can be considered as a single central cell and $N = 7$ ARC cells with the same width of the barriers and wells as the central cell, but with the barrier heights decreasing in accordance with a gaussian law. (This would be achieved by reducing the *Al* content $x < 0.45$.) The average transmissivity of their filter is $\tau_G = 0.84$. A major difference from our design, is that their cells do not have a common Bragg energy: rather it is the upper band edge which is common. This occurs because the narrow barriers of width $b = 1.5$ nm are effectively delta functions, and eq. 33 applies. All cells have the same width $d = b + w$, and therefore the same upper band edge. This property degrades the performance significantly for $E > 70$ meV. After the mid point of the band, their curve shows oscillations of increasing amplitude, with a deep minimum of $|t|^2 \sim 0.42$ at 90 meV, and a narrow peak at 93 meV, close to the upper band edge. A similar disease is seen in the drawings of Tung and Lee [7,8]. Even our single cell ARC with $\tau_1 = 0.81$ gives comparable performance. Fig. 6 compares the transmission curve for the gaussian filter with ours; in (a) we show the $N = 1$ and 4 cell systems and in (b) the $N = 2$ and $N = 3$ ARC cells. It is seen that the dips near the band edge become progressively shallower and further apart as the number of ARC cells N increases leaving a wider flat band in the middle. Despite having many fewer cells, as sketched in Fig. 4, our ARC designs show improvement in transmissivity and shape of the transmission curves. From a practical point of view they should be easier to fabricate reliably.

Comparing parts (a) of Figs. 3 and 5 one sees two effects of increasing K from three to five: the additional oscillations mentioned above, and the sharper definition of the band edges. Since the total length of the device is a consideration, ($\sim 2N + K$), there is a trade-off to be made between increasing N for higher transmissivity, and increasing K for sharper cut-off at the band edges.

VI. CONCLUSION

We have shown how to design an efficient band-pass filter for electrons in semiconductors. Transmission through a superlattice with even a few periods is almost zero in the forbidden bands and is characterized by a sequence of narrow resonances oscillating between an envelope of minima and 100% in the allowed bands. The role of an efficient antireflection coating is to push up this envelope of minima as close to 100% as possible, over as much of the allowed band as possible.

Our solution is facilitated by the use of Kard's parameterization of the transfer matrix in terms of trigonometric and hyperbolic functions. Using this representation, we have derived stability conditions which optimize an N-cell antireflection coating for an arbitrary initial superlattice. Numerical examples, using up to four cells in the ARC, show the possibility of increasing the overall transmissivity through the allowed band of a typical semiconductor superlattice up to 95%, while keeping the total width of the device to a minimum.

APPENDIX A: ADEQUACY OF QUARTER-WAVE COATING FOR ARC

Although it is well-known that quarter-wave ARCs work, it may be of interest to give a simple demonstration that they apply to our system. We can divide a multilayered ARC coating $v_i(x)$, with constant potentials in each layer, into a finite number N of symmetrical cells with potentials $a_N(x)$, $.a_{N-1}(x)$, ..., $a_1(x)$. We argue iteratively, so let us denote the potential of all cells except the last by $y(x)$. According to the above separation, the potential $y(x)$ consists of $N-1$ symmetrical cells, but is not necessarily symmetric itself. Then, the transfer matrix for the ARC coating can be factorized as $A = Y\,B$, where Y and B are the transfer matrices for potentials $y(x)$ and $a_1(x)$ respectively. In terms of matrix elements this relation takes the form

$$\begin{pmatrix} a_{11} & a_{12} \\ a_{21} & a_{22} \end{pmatrix} = \begin{pmatrix} y_{11}b_{11} + y_{12}b_{21} & y_{11}b_{12} + y_{12}b_{22} \\ y_{21}b_{11} + y_{22}b_{21} & y_{21}b_{12} + y_{22}b_{22} \end{pmatrix} . \tag{A1}$$

The first condition of eq. (10) can now be written as

$$\begin{aligned} &(y_{22}y_{11} + y_{21}y_{12})(b_{21}b_{11} - b_{12}b_{22}) \\ &+ y_{21}y_{11}(b_{11}^2 - b_{12}^2) + y_{12}y_{22}(b_{21}^2 - b_{22}^2) = 0. \end{aligned} \tag{A2}$$

Taking into account that the parameterization (10) is valid for B, the previous equation can be expressed as

$$\begin{aligned} &(y_{21}y_{11} - y_{12}y_{22})\cos 2\phi_1 - i\,((y_{22}y_{11} + y_{21}y_{12})\sinh\mu_1 \\ &+ (y_{21}y_{11} + y_{12}y_{22})\cosh\mu_1)\sin 2\phi_1 = 0. \end{aligned} \tag{A3}$$

An obvious solution is given by

$$\begin{aligned} y_{21}y_{11} - y_{12}y_{22} = 0 \quad &\text{and} \\ \cos\phi_1 = 0\,. \end{aligned} \tag{A4}$$

The first condition in (A4) is identical to the first condition in (10), but for the potential $y(x)$. Continuing in this way by induction, we will come to the point where the analogous condition is required for the last cell $a_N(x)$, which is equivalent to the condition $\cos\phi_N = 0$, as the cell $a_N(x)$ is symmetric itself. Therefore, one possible way to satisfy the first requirement in (10) is to take all $\cos\phi_p = 0$ at the design energy.

Acknowledgements

We are grateful to NSERC-Canada for discovery grant SAPIN-3198 (DWLS, GVM) and to DGES-Spain for continued support through grants PB97-0915 and BFM2001-3710 (JM). This work was carried out as part of CERION, Esprit project EP-27119 funded by the EU.

[1] G.V. Morozov, D.W.L. Sprung and J. Martorell, J. Phys. D (Applied Phys.) **35** (2002) (in press).

[2] C. Pacher, C. Rauch, G. Strasser, E. Gornik, F. Elsholz, A. Wacker, G. Kießlich and E. Schöl, Appl. Phys. Lett. **79** (2001) 1486. See also C. Pacher *et al.*, Physica E **12** (2001) 285.

[3] P. G. Kard, Optika i Spektr. **2** (1957) 236-44.

[4] I. Gomez, F. Dominguez-Adame, E. Diez, and V. Bellani, J. Appl. Phys. **85** (1999) 3916.

[5] D.W.L. Sprung, Hua Wu and J. Martorell, Am. J. Phys. **61** (1993) 1118.

[6] C.C. Chang and C.S. Kou, J. Phys. D (App. Phys.) **32** (1999) 139-146.

[7] Hsin-Han Tung and Chien-Ping Lee, IEEE J. Quantum Electron. **32** (1996) 507-12.

[8] Hsin-Han Tung and Chien-Ping Lee, IEEE J. Quantum Electron. **32** (1996) 2122-7.

[9] Q.K. Yang and A.Z. Li, J. App. Phys. **87** (2000) 1963-7.

TABLE I. Parameters for ARC cells using delta-function potentials

case, N	cell, p	μ_p	Ω_p, nm^{-1}	d_p, nm
1	1	1.00	0.61	4.71
2	1	1.71	1.39	5.38
	2	0.71	0.40	4.30
3	1	1.91	1.72	5.50
	2	1.45	1.05	5.18
	3	0.54	0.30	4.03
4	1	1.97	1.83	5.53
	2	1.79	1.58	5.43
	3	1.26	0.84	5.00
	4	0.44	0.23	3.85

TABLE II. Parameters for ARC cells using square potentials

Case N	cell p	μ_p	V_p, meV	b_p, nm	w_p, nm
1	1	0.63	344.6	0.73	5.60
2	1	1.04	279.0	1.50	5.80
	2	0.41	245.2	0.65	5.10
3	1	1.18	333.9	1.46	6.10
	2	0.83	294.6	1.13	5.70
	3	0.28	182.4	0.60	4.80
4	1	1.23	339.7	1.50	6.15
	2	1.07	326.1	1.34	6.00
	3	0.67	317.8	0.85	5.60
	4	0.20	137.1	0.58	4.60

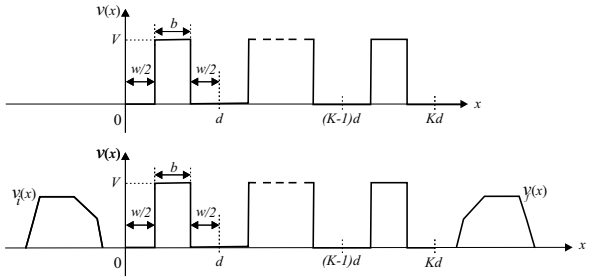

FIG. 1. Schematic drawing of a one-dimensional periodic array of quantum wells/barriers with cell width $d = w + b$ and height V; upper figure - no ARC coating; lower figure - with an ARC coating on each side of the array.

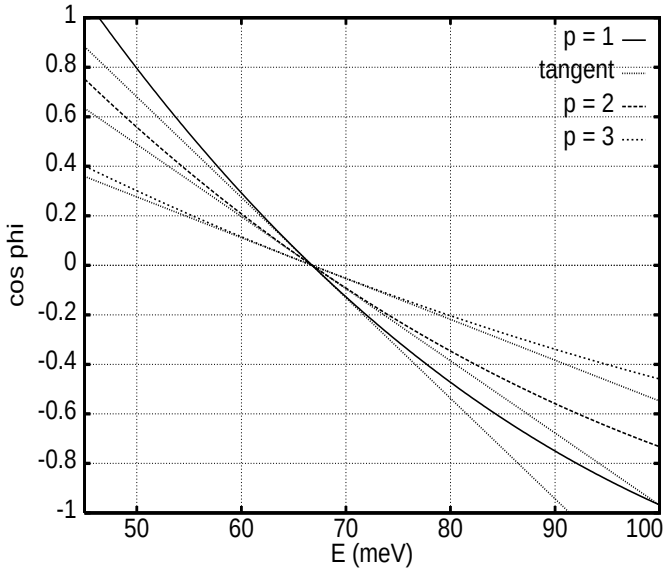

FIG. 2. $\cos\phi_p$ and their tangents at the multi-Bragg point (dotted lines) for the N= 3 ARC with square barrier cells.

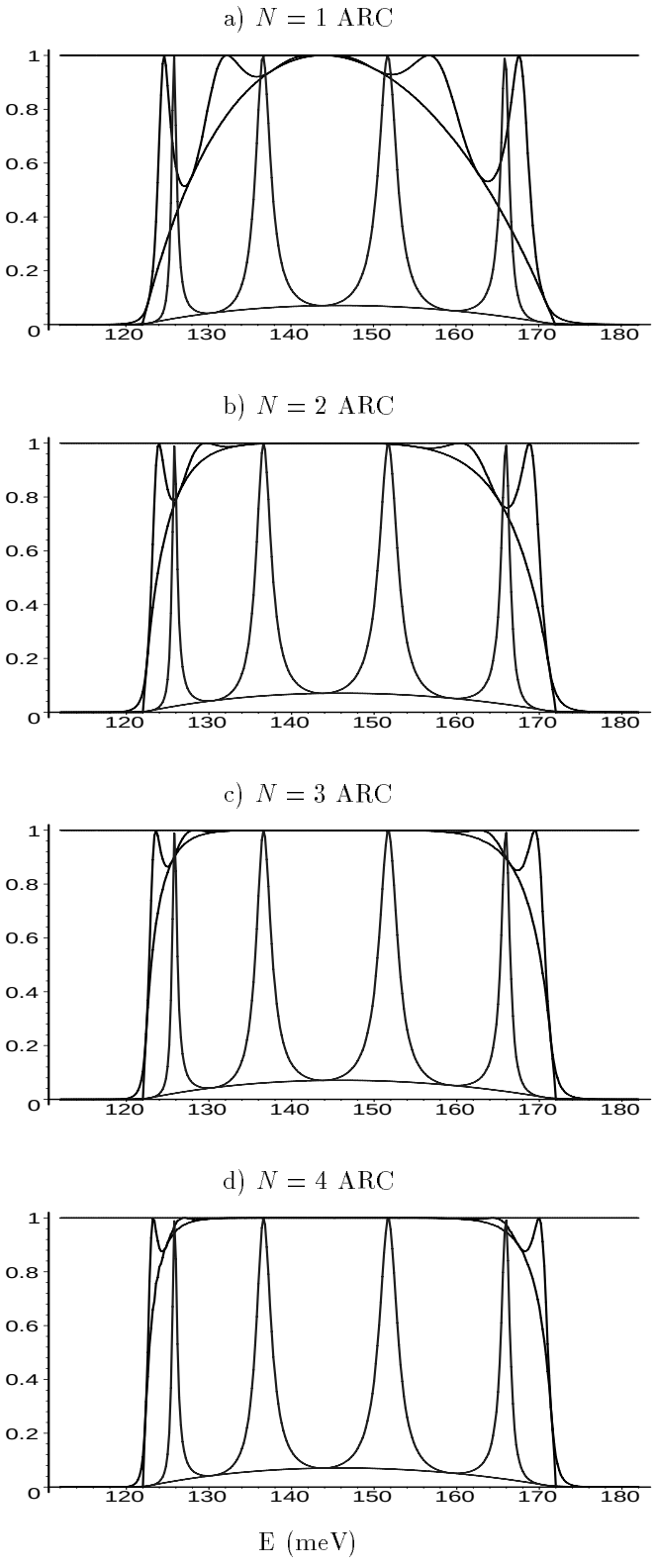

FIG. 3. Comparison between transmission probability vs. energy in the first allowed band of a superlattice with $K = 5$ deltas of strength $\Omega_c = 1.88$ nm^{-1} and period $d = 5.55$ nm without ARC, and with an N-cell ARC. The parameters of all ARC cells are given in Table 1. The envelope of minima is shown in all cases.

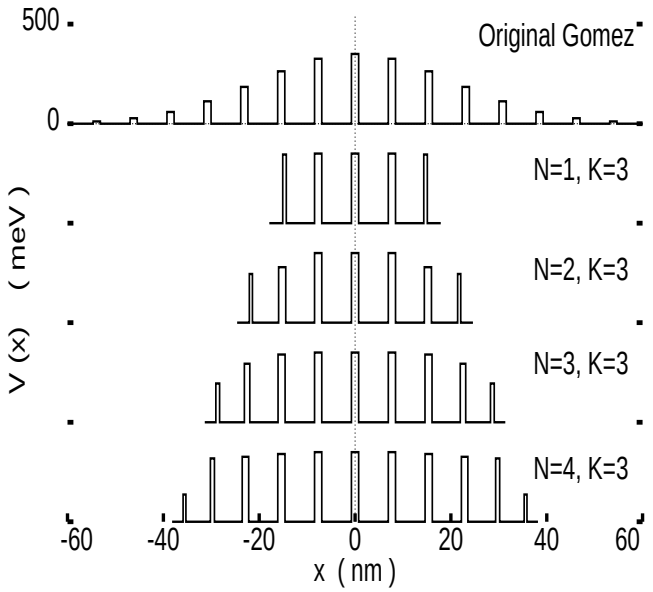

FIG. 4. Sketch of the gaussian array of ref. 4, and our four ARC solutions.

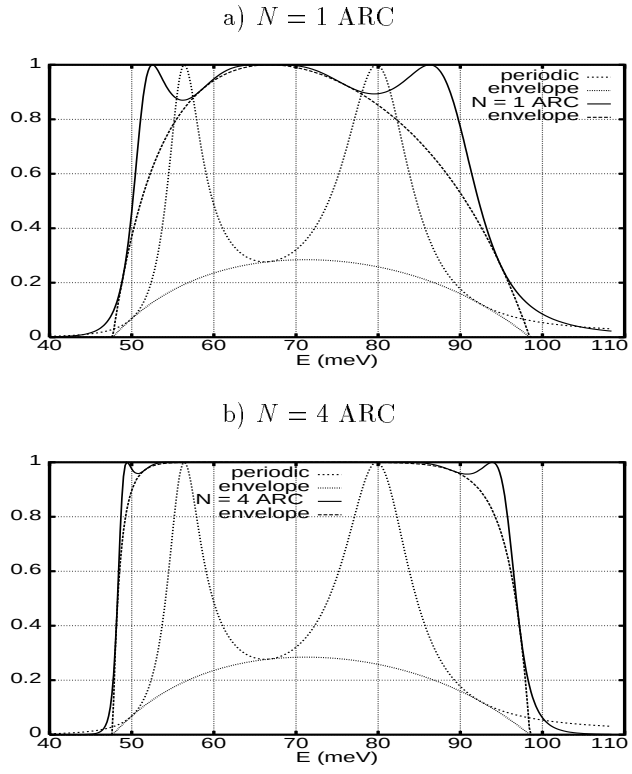

FIG. 5. Comparison between transmission probability vs. energy in the first allowed band of a superlattice with $K = 3$ square barriers of height $V = 350$ meV, barrier width $b = 1.50$, and well width $w = 6.20$ nm without ARC, and with an ARC. The corresponding envelopes of minima are shown for each curve. For parameters see Table 2.

a)

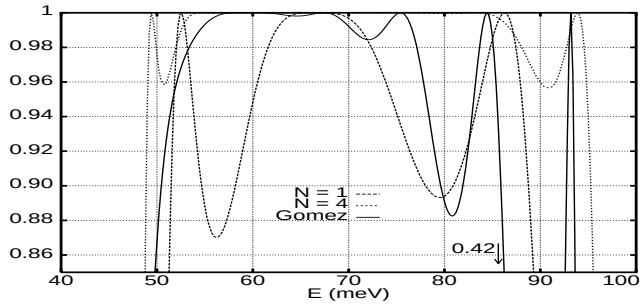

b)

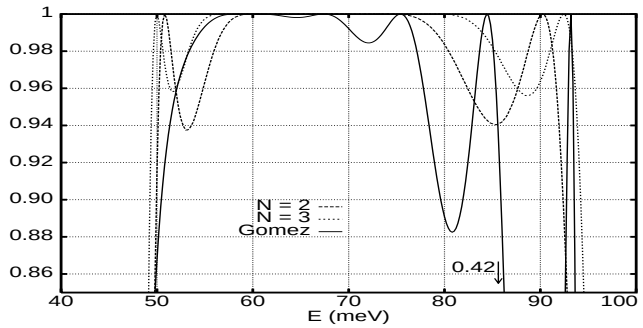

FIG. 6. Gomez et al.'s transmission compared to (a) $N = 1$, 4 and (b) $N = 2$, 3 ARCs.